

Polarization-Induced Anisotropic Phonons at Ferroelectric-Insulator Interfaces

Chaitanya A. Gadre¹, Xingxu Yan^{2,3}, Xiaoqing Pan^{1,2,3}

¹Department of Physics and Astronomy, University of California-Irvine, Irvine, CA, United States

²Department of Materials Science and Engineering, University of California-Irvine, Irvine, CA, United States

³Irvine Materials Research Institute, University of California-Irvine, Irvine, CA, United States

Atomically controlled interfaces of complex oxides offer new opportunities for nanodevice applications. Specifically, ferroelectric materials such as BiFeO₃ (BFO) have emerged as one of the forerunners for potential applications in nanoscale memories and other operating electronics by exploiting its polarization switching. Additionally, charge compensation at interfaces between perovskites leads to the emergence of two-dimensional electron/hole gases (2DE/HG) at ferroelectric-insulator interfaces with a spatial extent of a few nanometers [1-2]. The termination of polarization in the ferroelectric at the interface is counteracted by the electrostatic potential increase leading to the formation of 2DE/HG. Although these nanoscale phenomena have been thoroughly researched for their viability in operating electronics, thermal management is equally crucial and has not been investigated at the nanoscale. Where optical methods lack the necessary spatial resolution to study individual interfaces, vibrational EELS (VibEELS) emerges as a powerful tool for probing phonons at the nanoscale [3] and even atomic regimes [4]. Recently, vibEELS has been used to probe single defect modes such as point defects [5], stacking faults [6], and the specularity of semiconductor interfaces [7]. Armed with this technical capability, we demonstrate the detection of polarization-induced phonon modulation as well as the existence of anisotropic phonons at ferroelectric-insulator interfaces.

While the BFO unit cell retains its pseudo cubic structure, large scale polarization induces a shift of the cation as well as a tilt of the oxygen octahedra. Modulation of phonon properties by octahedral tilts has already been demonstrated [8] but changes due to cation displacement has yet to be investigated. As a result, it becomes necessary to characterize this structure change in terms of vibrational properties. Our system consists of a 100nm thick BFO film grown on TbScO₃ (TSO) producing large, 100 nm-wide domains (Fig 1A). In order to eliminate long-range polaritonic signals and isolate local phonon structure, we employ a dark field vibEELS (DF VibEELS) beam-detector geometry [5] as shown in Fig. 1B. We also use a 10mrad wide probe to allow for a greater portion of elastic scattering and limit EELS aberrations. This allows us to minimize the post-specimen tilt thereby maximizing the energy resolution and the quality of our acquired data. Fig. 1C shows three DF vibEEL spectra from the left and right domains, and TSO. While the spectral difference between BFO and TSO is drastic, the polarization-induced changes are more nuanced. The energy range above 12 meV (3 THz) is dominated by contributions from Fe and O to the total phonon density of states (PDOS) [9]. The Fe contribution is strongest from 12meV to 45 meV consistent with the spectral discrepancy illustrated in Fig. 1C.

Unexpectedly, the specific Fe displacement along a particular direction generates anisotropy in momentum space i.e., there is preferential phonon scattering. The existence of 2DE/HG also imposes further anisotropy that warrants detailed exploration. Fig. 2B shows the positions of the 25mrad EELS collection aperture with respect to the central beam. The vibrational mapping in Figs. C-D reveal anisotropic phonons wherein their amplitudes depend on their location in momentum space. Unexpectedly, the mappings show an opposite trend at the 2DE/HG suggesting that the free charge

carriers flip the anisotropy of the phonons in this region. This is more clearly represented in the line plot in Fig. 2E. The intensity of Y_+ and Y_- switch after the BFO-TSO interface and again after the 2DE/HG interface. This suggests symmetry breaking at each interface: ferroelectric-insulator interface and 2DE/HG-bulk interface. This surprising outcome offers an opportunity to probe the fundamental physics of nanoscale electron-phonon interactions as well as delivers insight into the propagation of phonons at complex-oxide interfaces. Study of these mechanisms informs the thermal-structure correlations of operating ferroelectric memory devices and aids in their optimization [10].

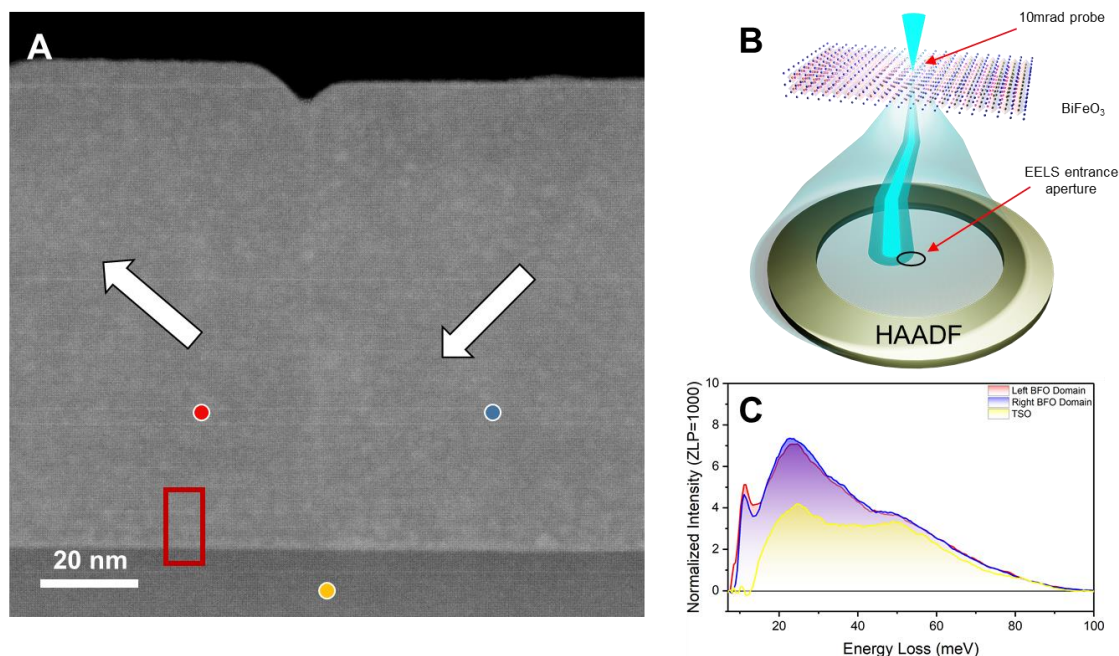


Figure 1: Vibrational Spectra of Polarized Domains in BFO. **A.** HAADF image containing two domains and TSO substrate. The arrows indicate direction of polarization. **B.** DF VibEELS beam-detector geometry. While the central beam escapes the EELS collection aperture, the neighboring diffraction spots (denoted by the immediate darker outer cone) offer significant elastically scattered electrons that contribute to a strong ZLP. This allows for the efficient tuning of the energy resolution and sufficient intensity of vibrational signals. **C.** DF VibEELS spectra at the locations marked in **A**. The spectra of the two domains have the strongest departure in the 12–45 meV energy range corresponding to strong Fe and O contributions to the total phonon signal.

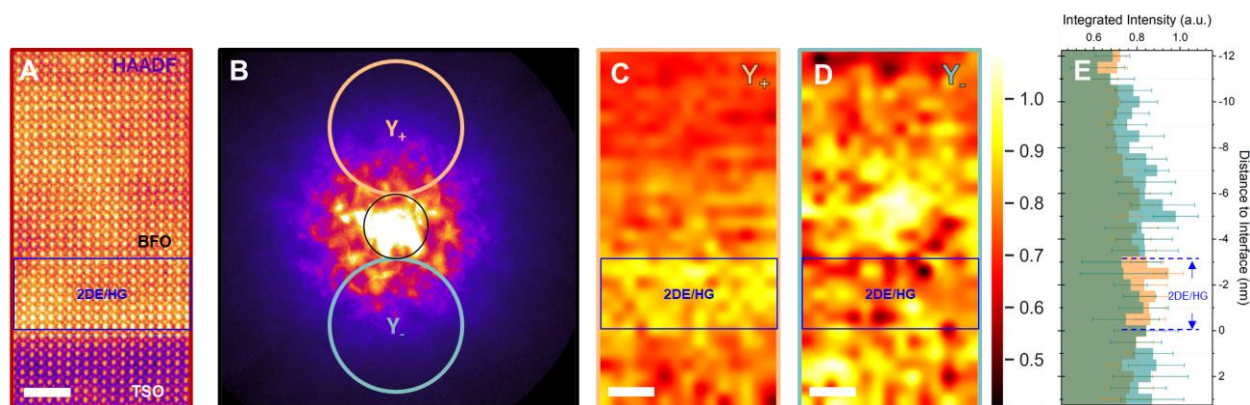


Figure 2: Anisotropic Phonons at a BFO-TSO interface. **A.** HAADF containing BFO and TSO with the 2DE/HG region marked in blue. This map region corresponds to the red box in Fig. 1A. The scale bars denote 2 nm. **B.** Convergent beam electron diffraction pattern using a 10mrad probe. The regions labeled Y_+ and Y_- correspond to locations of the EELS entrance aperture where the DF VibeEEL spectra were acquired. **C-D.** DF VibeEELS vibrational maps showing clear anisotropy. The 2DE/HG region is slightly larger than reported previously likely due to the poorer spatial resolution of the 10 mrad probe. **E.** horizontally averaged line profiles of maps in **C** and **D**. The dominating intensity switches at each interface: BFO-TSO interface, 2DE/HG-bulk interface.

References:

- [1] K Song et al., *Nature nanotechnology* **13** (2018), p. 198.
- [2] Y Zhang et al., *Nature nanotechnology* **13** (2018), p. 1132.
- [3] OL Krivanek et al., *Nature* **514** (2014), p. 209.
- [4] FS Hage et al., *Physical review letters* **122** (2019), p. 016103.
- [5] FS Hage et al., *Science* **367** (2020), p. 1124.
- [6] X Yan et al., *Nature* **589** (2021), p. 65.
- [7] C Gadre et al., *Microscopy and Microanalysis* **27** (2021), p. 1204.
- [8] ER Hoglund et al., *Nature* **601** (2022), p. 556.
- [9] Y Wang et al., *Acta Materialia* **59** (2011), p. 4229.
- [10] This work was primarily supported by the Department of Energy (DOE), Office of Basic Energy Sciences, Division of Materials Sciences and Engineering under Grant No. DE-SC0014430, and the National Science Foundation Materials Research Science and Engineering Center program through the UC Irvine Center for Complex and Active Materials (DMR-2011967).